This is a non-peer reviewed preprint

# Characterising strong force networks produced during granular shear using percolation methods: Revealing the bridge between local grain scale processes and macroscopic sliding

**Karen Mair[1], Espen Jettestuen[2] & Steffen Abe[3]**

[1] Njord and Department of Geosciences, University of Oslo, Norway;

[2] NORCE Norwegian Research Centre AS, Norway;

[3] Institute for Geothermal Resource Management, Bingen, Germany.

(Date: 5 April 2019)

(Corresponding author: karen.mair@geo.uio.no)

## Abstract

Faults, landslides and subglacial till often contain accumulations of granular debris. Their macroscopic motion is at least to some extent determined by the processes operating in this sheared granular material. A valid question in these environments is how the local behaviour at the individual granular contacts actually sums up to influence macroscopic sliding. Laboratory experiments and numerical modelling can potentially help elucidate this. Observations of jamming and unjamming as well as concentrated shear bands that appear to scale with grain size, suggest that a simple continuum description may be insufficient to capture important elements of the behaviour. We therefore seek a measure of the organisation of the granular fabric and the structure of the load bearing skeleton that shows how the individual grain interactions are summing up to influence the macroscopic sliding behaviour we observe. Contact force networks are an expression of this. We choose to investigate variability of the 'important' or most connected system spanning strong force networks produced in 3D discrete element models of granular layers under shear. We use percolation measures to identify, compare and track the evolution of these system spanning contact force networks. We show that the geometries and interactions of these load bearing structures, reflected as specific topological measures, are

sensitive to size (and likely shape) distribution of the granular material. Importantly, distinct (measurable) changes in the topological structural characteristics of strong force networks with accumulated strain are directly correlated to fluctuations in macroscopic shearing resistance. This illustrates the sensitivity of 3D force networks to details of granular materials (such as size and shape distribution) and also the important bridging role they play between individual grain scale processes and macroscopic sliding behaviour.

## Introduction

Active geological faults as well as landslides, rockslides, debris avalanches and sub glacial tills contain accumulations of granular debris subjected to normal load and shear. The response of the granular material to the applied loads controls the rheology and hence sliding friction of the system and thus is crucial to understand.

Studies of the physics of jamming (and unjamming) reviewed in (Behringer and Chakraborty, 2019) indicate that sheared granular material can support finite amounts of stress and strain with little obvious motion but that under large enough stress or strain, the material will yield, deform or flow in a dynamic way (eg. Herrera et al., 2011; Dapeng et al., 2011). The switch between the 'stuck' (jammed) and 'flowing' (unjammed) states is often referred to as the jamming/unjamming transition (Majmudar et al., 2007; Vinutha and Sastry, 2019). It would be convenient if all the grain contacts failed as a continuum but observations of jamming as well as localised shear band fabrics (e.g. Roscoe, 1970; Mühlhaus and Vardoulakis, 1987) with roughly fixed widths of a few (5-10) grains, suggest a continuum description is insufficient to explain the behaviour. Since bulk deformation is clearly not disconnected from the grain scale, we must consider grain scale processes and crucially, how the behaviour at individual and groups of grain contacts sums up to affect the bulk rheology.

When subjected to remote loading, the forces acting between neighbouring grain-grain contacts depend on the geometry of contacts and the surrounding granular environment and can be highly variable (e.g. Oda et al., 1982, Howell et al, 1999, Mair and Hazzard, 2007). Typically, the

average applied stress is very unevenly supported, with some contacts bearing much higher than average forces whilst others enjoy lower that average forces (Cates et al. 1998; Howell et al., 1999). This has several implications: i) local stresses on particular grain contacts can be much larger than would be expected given the remote applied stress and as a consequence, parts of the granular material become geometrically 'stuck' or 'jammed'; ii) in contrast, other regions encounter much lower than average forces so individual grains are potentially much more mobile and susceptible to rearrangement; and iii) local parts of the system may reach fracture or yield thresholds at significantly lower applied loads than expected. Examples include observations of so called 'cracked pebbles' in granular beds fracturing at lower than expected mean stress, indicating higher than average forces are reached at some contact (e.g. Taboada et al. 2015).

The population of contact forces in a granular system is typically subdivided into 'strong' contact forces where $F/F_{mean} > 1$ and 'weak' contact forces where $F/F_{mean} < 1$ (eg. Radjai et al., 1996; Radjai et al., 1998; Radjai et al., 1999; Meuth et al., 1998). Strong forces have been shown to be more preferentially oriented than weak forces (eg. Majmudar and Behringer, 2005; Daniels and Hayman, 2008; Mair and Hazzard, 2007) and their population distributions have been linked by various investigators with jamming transitions (Li and Nagel, 1998, 2010; Majmudar et al., 2007). Strong force populations also appear to be sensitive to grain size distributions (Mair and Hazzard, 2007). Although strong force populations have received most attention and as such are the focus of our study, we note that weak forces may play a crucial role as either passive stabilizing agents or an active force network alternatively 'propping up' the strong contacts or conversely allowing them to buckle and fail (eg. Aharanov and Sparks, 2004; Arévalo et al., 2010; Azema and Radjai, 2012).

As an ensemble, heterogeneous contact forces can form spatially connected networks that are often referred to as grain bridges or force chains (eg. Sammis et al. 1987; Sammis and Steacy, 1994) and can potentially span the entire system. As with the individual contact forces themselves, they are subdivided into strong force networks ($F/F_{mean} > 1$) thought of as the "strong backbone" of a granular system and weak networks (with $F/F_{mean} < 1$). The networks are intimately related but have distinct properties and ultimately quite different roles as mentioned above. Importantly, although elements of these networks, in particular, their patterns and

orientations, are persistent during shear, participation in the networks appears to be highly transient, with individual grains serially belonging to both strong and weak force networks during their life cycle.

When considering the force networks, two characteristics may feasibly be thought to be critical: i) the size of largest force generated and ii) the connectivity of the strong force system. The size of the largest force could certainly be significant in terms of inducing local fragmentation or yielding (at macroscopic loads smaller than expected) but due to its local nature, its halo of influence may not extend to the edges of the system and thus influence on macroscopic sliding behaviour may be limited. In contrast, we anticipate that the meso-scale structures and in particular the degree of connectivity of the strongest contact forces could rather be a key player controlling the macroscopic sliding. Here we focus on the details of strong system spanning force networks since we believe they have the highest potential to control macroscopic rheology.

Three dimensional numerical models of granular shear, have shown (qualitatively) that the grain size characteristics of the granular material affects the style of strong force networks (Mair and Hazzard, 2007). Such ideas had previously been proposed for 2D systems (Oda et al. 1982, Howell et al., 1999), and the concepts inherent had also earlier been invoked (Cates et al., 1998) to explain intriguing mechanical data obtained from 3D laboratory experiment on sheared granular layers having different grain size distributions or grain shapes (Cates et al., 1998; Mueth et al. 1998, Mair et al. 2002). Here, using 3D numerical modelling and quantitative network structural analysis measures, we build on this 2D work and 3D qualitative observations and interpretations, to highlight how force networks may develop and evolve for a range of conditions and importantly how they relate to macroscopic mechanical behaviour of sheared granular materials.

# Methods

*Granular shear models*

Our 3D numerical simulations of granular shear (Figure 1) consist of unbonded (and unbreakable) spherical particles sheared between solid boundaries at the top and bottom. The model is constructed using the discrete particle method (e.g. Cundall and Strack, 1979) and in particular, the software engine 'ESyS-Particle 3D' (e.g. Abe et al. 2004). We employ repeating boundaries left and right, and frictionless walls front and back. Constant normal load is applied and maintained in the z-direction (vertical) then shear is applied in the x-direction as indicated by arrows. Upon loading, the individual particles interact with their nearest neighbours according to simple normal elastic interactions and frictional contact laws. Simulation conditions used in this study are summarised in Table 1. To investigate the influence of geometry and applied load on developing force networks, we conduct a suit of simulations for different geometries (varying particle size distribution or mean particle diameter) and different normal stresses (5 MPa, 15 MPa, 30 MPa).

Despite some obvious limitations, this method lends itself very well to simulating granular shear due to its discrete nature (Mora and Place, 1998; Aharonov and Sparks, 1999; Morgan, 1999). A highly attractive feature of such an approach is the internal visualisation it affords. The individual grain scale motions and contact force interactions, as well as ensemble behaviour and the macroscopic mechanical response 'felt' at the boundaries of the model (fault walls) can all be tracked synchronously with accumulated strain. Although we have previously feted the importance of grain fracture in simulating faulting processes in a realistic way (e.g. Abe and Mair, 2005; Abe and Mair, 2009; Mair and Abe, 2011, Heilbronner, and Keulen, 2006), here we switch off this feature and invoke the simpler case of non-fracturing grains to demonstrate the feasibility of using percolation measures as a structural analysis method. Importantly, however, we are using established proven tools and a methodology and workflow that has been strongly validated experimentally over the last few years (eg. Abe and Mair, 2009; Mair and Abe, 2008; Mair et al. 2002). Even without grain fracture, by interrogating different grain geometry endmember cases, we can indirectly comment on the effect changes in grain size or shape would have on force network characteristics.

*Loading and mechanical response*

Normal load is applied in the z-direction to the upper and lower boundaries of the simulated granular material, then after equilibrating is kept constant as a constant shear displacement is applied in the x-direction. Friction is nominally described as shear stress divided by normal stress and is generally presented as a function of engineering shear strain. Shear strain is calculated from the incremental displacement in x direction divided by the initial layer thickness. The (micro)parameters used in the numerical simulations (Table 1), are chosen to correspond to those of previous granular shear simulations (Mair and Hazzard, 2007). Importantly, both sets of simulations have been thoroughly validated by comparison with laboratory direct shear experiments (Mair et al., 2002; Abe and Mair, 2009).

*Contact forces*

During shear simulations, we extract the total force acting between pairs of neighbouring particles as a vector located at the contact point between particles. This vector will have a normal and shear component, however, for the purposes of this paper we do not decompose into normal and shear forces. A snapshot of the contact forces developed in a typical granular shearing simulation after 100% shear strain (engineering shear strain = 1) is presented in Figure 2. There is a clear preferred orientation of larger forces into two 'chains', oriented obliquely to the shearing direction, that carry enhanced force across the granular layer. Further details on the orientations of contact forces are presented in the results section.

*Percolating force chains*

A key goal of this paper is to demonstrate the relationship between the most important system spanning force networks and the macroscopic sliding resistance of our sheared granular systems. A crucial first step is therefore to carry out a structural analysis of force networks developed, identify the most 'important' or system spanning strong force chains and investigate how they evolve and relate to macroscopic sliding friction measured at the boundaries of the system. For this, we utilise tools from the complex networking community (after Ostojic et al., 2006) to investigate the connectivity of forces. A recent review (Bassett et al., 2015) provides an excellent overview and evaluation of the various network measures and methods available. Percolation is

the theory of connectedness and is often invoked to denote a threshold where flow through porous media reaches from one side of a body to the other. Once a percolating structure has been identified, its topology can be usefully characterised and compared using a suit of Percolation measures. Here, we borrow this concept to identify and characterise system spanning strong force chains developed in our 3D sheared granular systems.

We define the Percolation threshold as the force threshold (between individual particles) where a chain of connected forces first percolates (i.e. transcends) the sample from upper to lower boundaries (Figure 3). A key reason to use percolation measures is to characterise the connected force network structure in a straightforward and unambiguous way. They appear to be a useful way to compare connected networks for different psd granular systems and to demonstrate the links between 3D force configurations and macroscopic shearing resistance. If the force, F, between two particles is greater than $F_t$ (a threshold value), then that force is included in the network. The resulting network is defined as percolating if it connects the upper and lower boundaries of the model. $F_c$ is the percolation threshold i.e. the maximum value of $F_t$ where a network first percolates. An example of a percolating (red) and non percolating (white) force cluster are shown in Figure 3.

For each snapshot of our simulations, we search the entire contact force population in terms of magnitude, starting at high F so initially our 'network' just includes the few very large contact forces. We systematically reduce the $F_t$ until we hit $F_c$ percolation when we first get a connection between upper and lower boundaries of model. This then gives us a useful way to identify and characterise 'important' force network. We can potentially do this at every time step (or for a sequence of snapshots separated by a specific time increment) and look at evolution of the geometry, number of contacts, branching, distribution of force magnitude of percolating structures as the interconnected force network evolves with accumulated shear.

The significance of this percolation measure is that it focuses on the structural organisation of the larger contact forces rather than just the magnitude since even if you have isolated high forces, although they may cause isolated fragmentation, it is unclear whether their effects would extend to the boundaries and directly affect macroscopic sliding. Characterisation and structural

analyses of the force networks identified in our granular shear simulations, including contact Force ($F_{max}$, $F_{mean}$), percolating force threshold ($F_c$) and number of particle involved in the percolating chain (K+1) is summarised in *Table 2. Percolation measures*.

## Results

Mechanical and structural data collected from typical granular shear simulations, for conditions summarised in Table 1, are now presented below (Figures 4 - 8).

*Friction*

Macroscopic mechanical behaviour of a typical simulation is plotted as friction (shear stress/normal stress) versus shear strain in Figure 4. Friction plots for other simulations are summarised in Table 1. An approximately steady state mean friction level of ca. 0.36 is reached after ca. 0.2 strain with fluctuations in friction characterised by a standard deviation of ca. 0.025. A similar mean friction value is obtained for simulations conducted on varying psd granular systems and only a small influence of normal stresses is observed (Table 1; Mair and Hazzard, 2007). Fluctuations in friction however, do appear to sensitive to mean grain size with respect to simulation size (i.e. number of particles), with larger (fewer) particles leading to greater fluctuations and (high frequency) fluctuations are also slightly reduced at higher normals stress. The mean friction value observed in all the simulations presented is lower than might be expected for shear of a real rock gouge, however it is entirely consistent with friction measured in previous numerical modelling observations (Abe and Mair, 2009) and more importantly, matches very well with friction values obtained from laboratory shear experiments of spherical glass beads under similar 'non-fracturing' conditions (Mair et al., 2002; Mair and Abe, 2011). The red box marks the period which is highlighted in more detail below.

*Contact force orientations*

The orientations of strong contact forces weighted by magnitude are plotted as polar histograms in Figure 5. Two projections are presented, a) a side view (in the x-z plane) exposing the shear direction (top to the left) and b) the top view (x-y plane) parallel to shear (left-right). The data

presented consist of the strong contact forces (those with $F/F_{mean}>1$) developed during the period of shear strain from 0.66 to 0.8 that corresponds to the boxed area in Figure 4. This is a period of strain where a significant perturbation in macroscopic friction is observed. The variation with increasing shear strain is indicated in the histograms by the shaded colour bar (progressing from dark to light grey with increasing strain) and with the start and end highlighted by the red and blue arrows respectively. Consistent with the snapshot shown in Figure 2, data indicate stronger contact forces organising preferentially oblique to the direction of shear (Figure 5a) and also that strong forces are directed sub parallel to the shearing direction (Figure 5b). The greyscale colouring (from dark to light) indicates a transition from more directed contact forces (red arrow) with a relatively high (ca. 55 degree) angle with respect to shear direction, to slightly lower (ca. 35 degree) angle to shear (blue arrow) and hence more shallow forces following the drop in friction. Comparable polar histograms for contact force orientations produced in other simulations are presented in Supplementary material (and Mair and Hazzard, 2007) demonstrating that the first order observations for the specific period of strain highlighted in Figure 5 are general behaviour seen for a range of conditions and granular geometries.

*Percolating clusters and friction*

The connectivity of system spanning strong contact force networks, arguably the most important features, are now determined using Percolation methods. (K+1) is a topological measure that characterises the size i.e. number of particles participating in a percolating network and Fc is the percolation Force threshold (as described in methods section, after Ostojic et al., 2006). Data are presented for a typical simulation in Figure 6 and summarised for all simulations in Table 2. For simulation om015, the entire contact force network is interrogated using the method described above for the same shear strain window (0.66 - 0.8) already presented in Figures 4 & 5. K+1 and Fc are plotted along with macroscopic friction as a function of shear strain for this window (Figure 6a and 6b respectively). The key motivation here is to determine the nature of the percolating networks and investigate any correlations between their characteristics and macroscopic friction during the stress fluctuation observed. The data show a background base level of ca. 20 particles making up the system spanning chain that jumps to ca. 300 particles at shear strains of 0.7. This rather dramatic increase in the ‘size’ (or length) of the percolating cluster indicates that the dominant system spanning force network is, at least temporarily,

becoming significantly more diffuse. This change occurs at the same moment as a drop in macroscopic friction. As friction recovers to its mean value, the length of the percolating cluster gradually drops back to its background level indicating it has resorted to a more directed and focussed network. This observation intimates a direct link between microstructural organisation and macroscopic strength.

The structure of connected strong networks for other simulations is presented in Table 2. Data show that smaller grain sized simulations (having a larger number of particles) have systematically more particles involved in the percolating network - as would be expected since more particles are needed to even transcend the shear zone. Also, for higher normal stresses, the number of particles involved in the percolating network is systematically reduced. As shown in Table 2, this is inversely related to the percolating threshold $F_c$ which increases with normal stress.

In Figure 6b, we plot together the size of the percolating cluster (already shown in Figure 6a) alongside the percolating threshold force $F_c$ , i.e. the maximum value of $F_t$ where a network first percolates from top to bottom in the system. The force threshold $F_c$ associated with identifying the first (or strongest) percolating network displays a value of ca. 0.4 which temporarily drops to 0.27 before returning to original value. Notably, this change in force threshold displays an inverse relationship with the size of the percolating cluster indicating that magnitude of contact forces in the system spanning strong force network decrease (becoming more inclusive of a wider range of forces) as its style becomes more diffuse. Again, this change occurs simultaneously with a reduction in macroscopic friction highlighting a connection between microstructural accommodation of stress and the bulk system strength measured at the boundaries.

The force threshold values and size of the percolating clusters for other simulations are summarised in Table 2 and show that $F_{max}$, $F_{mean}$ and $F_c$ all increase systematically for larger applied normal stress. In addition, $F_{max}$, $F_{mean}$ and $F_c$ are larger in magnitude for simulations with larger grain size (i.e. where the same applied total load is concentrated on much fewer particles present in the simulation).

*Topology of percolating clusters as a function of particle size distribution*

We know, at least qualitatively, from Mair and Hazzard (2007), that the geometry of strong force networks is sensitive to particle size distribution (psd) and potentially the grain shape (Mair et al., 2002; Abe and Mair, 2009) of the granular material. Here, we identify 'important' force networks in an unambiguous way using percolation methods to reveal the influence of grain size on force cluster geometry.

We conduct a series of shearing simulations for two different granular materials, one having a narrow gaussian size distribution (Figure 7), the other with a power law size distribution (Figure 8). For each particle size distribution, at a snapshot (Engineering shear strain = 1), we determine the percolation threshold $F_c$ , equivalent to the maximum value of $F_t$ where a strong force network first percolates from upper to lower boundaries of the simulation. The values of the percolating thresholds are $F_c = F_t = 0.329$ and $F_c = F_t = 0.216$ for the gaussian, and power law size distributions respectively. The contact forces that participate in those percolating clusters are plotted in Figures 7a & b, and Figures 8a & b. (No other contact forces are plotted here). Note that due to the repeating boundaries in the model (right and left), although the network may appear in two pieces, it exits right and re-enters at the same position on the left so in fact comprises a single connected structure. Next, for exactly the same shear strain snapshots, we interrogate both geometries for the 'next largest' system spanning clusters, by determining the strong force structures that transcend the system in the vicinity of the percolation threshold (i.e. at $F_t$ slightly lower than $F_c$).

For the gaussian particle size distribution (Figure 7c-j), at $F_t = 0.309$ we encounter the next sets of system spanning strong force clusters. Colours indicate connected forces, so these independent (i.e. not connected) clusters are coloured differently from each other. On reducing $F_t$ , the original $F_c$ cluster (Figure 7a & b) is slightly enhanced (Figure 7c & d; white markers), then 3 additional and independent force clusters are identified (Figure 7e - 7j; blue, red, gold markers). Importantly these 4 system spanning networks share some common features. They all form distinct pipe like structures oriented oblique to direction of shear at an angle of ca. 55 degrees. In general they are quite self contained, staying away from each other and do not expand

significantly in the out of plane (y-direction). In a broad sense they approximate linear 1-D oblique structures.

For the power law size distribution, (Figures 8a-f), the percolating cluster first appears at $F_c = F_t = 0.216$. Above the percolation threshold (i.e. at Forces $F_t$ lower than $F_c$) no new discrete clusters are formed, but instead, the original percolating force network gradually extends in a tree like manner (Figures 8c-f). A preferred overall orientation oblique to shear is still prevalent, however, unlike the gaussian case above (Figure 7), these structures 'grow' much more out of plane (in the y-direction) and have strongly sheet like or 3-D characteristics.

Animations which illustrate the 3D nature of the force clusters presented in Figures 7 and 8 are included as Animation A1 and A2 respectively in the Supplementary material section.

## Discussion

The general mechanical results presented in this paper are consistent with previous 3D granular shear simulations (e.g. Mair and Hazzard, 2007; Abe and Mair, 2009) and validated by laboratory experiments (Mair et al., 2002; Frye and Marone, 2002). Although we use highly simplified geometries, where grain fracture is essentially switched off, we have laboratory validation experiments for this non-fracture regime (Mair et al. 2002), we know the effects grain fracture would have both structurally and mechanically (Abe and Mair, 2009), and we investigate endmembers having non-evolving but distinct grain size distributions (tn037g, tn021g, tn014f and tn032f) to reveal possible effects of progressive grain comminution that one would see as comminution progressed.

In terms of individual grain scale processes, the orientation and magnitude of the contact force population as a function of normal stress and grain size distribution are consistent with previous 3D numerical work (Mair and Hazzard, 2007), 2D observations (Radjai et al., 1996; 1999; Meuth et al., 1998 Aharonov and Sparks 2004; Howell et al., 1999) and theory (Cates et al., 1999).

Here, however, we focus mainly on connected force structures in an effort to discover a bridge between grain scale and system scale processes (Chivalo et al., 2012; Ness and Sun, 2015). We quantify strong forces using Percolation methods (after Ostojic et al. 2006). The main features of the system spanning force chains, characterized by the basic percolation measures, the percolation threshold ($F_c$) and percolation structure length (K+1) are presented for a series of shearing simulations. Their structure (length, mean F) depends on normal stress or grain size distribution in addition to the grain size (or number of particles in the simulation). There is consistency between repeat simulations carried out at comparable conditions demonstrating the reproducibility of the simulations and the robustness of results. As conditions (either applied stress or granular geometry) change, the Percolating force network structures adapt. The degree or persistence of such effects will be investigated in future work.

We demonstrate a strong correlation between evolving system spanning networks and macroscopic friction (Figure 4-6). This confirms the qualitative observations of 3D shear (Mair and Hazzard, 2007), inferences previously made and directly observed in 2D photoelastic experiments (see Howell et al, 1999; Behringer and Chakraborty, 2019; Daniels and Hayman, 2008) and numerical models (eg. Aharonov and Sparks, 2004). The fact that we see a direct link between percolating force networks and macroscopic friction demonstrates their important role in bridging between grain scale processes and bulk macroscopic sliding behaviour. We note the potential relevance of combining these observations to related work on the rheology and flow regimes of sheared granular materials highlighting the role of bridging structures (Chivalo et al., 2012; Ness and Sun, 2015).

Although we have focussed on the strong contact forces, the fact that they exist as fairly isolated structures (at least for the narrow grain size simulations), results in the significant potential for enhanced mobility in areas of low contact forces elsewhere. This has been cited as a potential mechanism for long runout (much longer than predicted) for very large landslides (eg. Davies and McSaveney, 2012) and could have crucial relevance to frictional stability in granular fault zones.

Importantly, we have demonstrated usefulness of using Percolation methods for unbiassed identification and characterisation of connectivity in force networks (after Ostojic et al. 2006). Topology has recently been used in various systems to quantify granular packings (Arévalo et al. 2010; Azéma and Radjai, 2012, Kondic et al., 2012). The alternative network measures are available to quantify sheared granular systems and have been excellently summarised in (eg. Basset et al., 2015). However, we propose due to its simplicity and effectiveness for the task, this method be implemented and basic percolation measures reported in future numerical investigations of force networks developed during shear.

One of the main limitations of this work in comparing directly to geological deformation scenarios, is clearly the lack of grain fracture in these simple simulations. The sites of high contact force could certainly be possible regions of enhanced grain fracture and fracture would lead to an evolution in grain size distribution. We have previously envisaged and discussed this scenario at length (Mair et al., 2002; Mair and Hazzard, 2007). and more recently reported on a range of simulations involving somewhat realistic grain fracture (Abe and Mair, 2005; Mair and Abe, 2008; Abe and Mair, 2009; Mair and Abe, 2011). A lengthier discussion is therefore deemed beyond the scope of this paper.

Our future work will investigate the details of force chain networks in sheared porous granular material having breakable grains (i.e. aggregates composed of many particles bonded together with breakable bonds) to reveal for example, what the nature of system spanning force networks immediately prior to and following fracture of grain.

## Conclusions

In this paper, we present details of contact force networks or ‘force chains’ produced in 3D simulations of granular shear for a series of normal stress conditions and grain geometries. We demonstrate how system spanning force networks can be characterised using percolation methods to allow straightforward but unambiguous identification, comparison and tracking of the structures as a function of shear strain and for different grain geometries or applied loads. We

show that the structure of system spanning force networks are highly sensitive to grain size distributions of the granular material. We also show direct correlation between changes in the structure of system spanning networks and fluctuations in macroscopic friction. This suggested that these chains are playing a fundamental role in bearing load across the shear zone and any breakdown or change in their style or nature such as might happen following grain fracture when grain size distribution evolves, will influence mechanical macroscopic behaviour.

## Acknowledgements

The simulations presented were performed on resources provided by UNINETT Sigma2 - the National Infrastructure for High Performance Computing and Data Storage in Norway. The authors thank Mark Naylor for stimulating discussions during this work and helpful comments on this manuscript.

## References

Abe, S., Place, D., and Mora, P. (2004), A parallel implication of the Lattice Solid Model for the simulation of rock mechanics and earthquake dynamics, Pure Appl. Geophys. 161, 2265–2277.

Abe, S., and Mair, K., (2005) Grain fracture in 3D numerical simulations of granular shear, Geophysical Research Letters vol 32, L05305, doi: 1029/2004GL022123

Abe, S. and K. Mair (2009), Effects of gouge fragment shape on fault friction: New 3D modelling results, Geophysical Research Letters, 36.

Aharonov E., and Sparks, D., (2004), Stick-slip motion in simulated granular layers, Journal of Geophysical Research, Vol. 109, B09306, doi:10.1029/2003JB002597

Arévalo, R., Zuriguel, I., & Maza, D. (2010). Topology of the force network in the jamming transition of an isotropically compressed granular packing. Physical Review E, 81(4), 041302.

Azéma, E., & Radjai, F. (2012). Force chains and contact network topology in sheared packings of elongated particles. Physical Review E, 85(3), 031303.

Bassett, D. S., Owens, E. T., Porter, M. A., Manning, M. L., & Daniels, K. E. (2015). Extraction of force-chain network architecture in granular materials using community detection. Soft Matter, 11(14), 2731-2744.

Behringer, RP. and B. Chakraborty, (2019), The physics of jamming for granular materials: a review, Rep. Prog. Phys. 82 012601

Cates, M. E., Wittmer, J. P., Bouchaud, J.-P. & Claudin, P., (1998), Jamming, force chains, and fragile matter. Phys. Rev. Lett. 81, 1841–1844

Chialvo, S., J. Sun, and S. Sundaresan, (2012) Bridging the rheology of granular flows in three regimes, Phys. Rev. E 85, 021305.

Cundall PA., and Strack, ODA. (1979), A discrete numerical model for granular assemblies, Geotechnique, 29, 47–65.

Daniels, K. E., and N. W. Hayman (2008). Force chains in seismogenic faults visualized with photoelastic granular shear experiments, J. Geophys. Res., 113, B11411, doi:10.1029/2008JB005781.

Dapeng B, J Zhang, B. Chakraborty & RP. Behringer, (2011), Jamming by shear, doi:10.1038/nature10667

Davies, T. R. H., and McSaveney, M.J. ( 2012), Mobility of long-runout rock avalanches, in Landslides: Types, Mechanisms and Modeling, pp. 50– 58, Cambridge Univ. Press, Cambridge, doi:10.1017/CBO9780511740367.006.

Heilbronner, R., and N. Keulen (2006), Grain size and grain shape analysis of fault rocks, Tectonophysics, 427, 199– 216

Herrera, M, S. McCarthy, S. Slotterback, E. Cephas, W. Losert and M. Girvan, (2011), Physical Review E, 83, 1.

Howell, D., Behringer, R., Veje, C., (1999), Stress fluctuations in a 2d Couette experiment: a continuous transition. Phys. Rev. Lett., 82 (26), 5241–5244.

Kondic, L., Goullet, A., O'Hern, C. S., Kramar, M., Mischaikow, K., & Behringer, R. P. (2012). Topology of force networks in compressed granular media. Europhysics Letters, 97(5), 54001.

Liu, A. & Nagel, S. (1998), Jamming is not just cool any more. Nature 396, 21–22.

Liu, A. J. & Nagel, S. R. (2010), Granular and jammed materials. Soft Matter 6, 2869–2870.

Mair, K. and S. Abe (2011). Breaking Up: Comminution Mechanisms in Sheared Simulated Fault Gouge, Pure and Applied Geophysics 168(12): 2277-2288.

Mair, K., and Abe, S., (2008), 3D numerical simulations of fault gouge evolution during shear: Grain size reduction and strain localization, Earth and Planetary Science Letters, 274, p72-81

Mair, K., K. M. Frye and C. Marone (2002). Influence of grain characteristics on the friction of granular shear zones. Journal of Geophysical Research-Solid Earth 107(B10).

Mair, K. and J. F. Hazzard (2007). "Nature of stress accommodation in sheared granular material: Insights from 3D numerical modeling." Earth and Planetary Science Letters 259(3-4): 469-485.

Majmudar, TS. and RP. Behringer, (2005), Contact force measurements and stress-induced anisotropy in granular materials, Nature, Vol 435, 23 June 2005.

Majmudar, T. S., Sperl, M., Luding, S. & Behringer, R. P. (2007). Jamming transition in granular systems. Phys. Rev. Lett. 98, 058001.

Meuth, D. M., Jaeger, H. M. & Nagel, S. R. (1998), Force distribution in a granular medium. Phys. Rev. E 57, 3164–-3169.

Morgan, (1999), Numerical simulations of granular shear zones using the distinct element method: 2. Effects of particle size distribution and interparticle friction on mechanical behavior, J. Geophys. Res., 104(B2), 2721– 2732.

Mühlhaus, H. B., & Vardoulakis, I. (1987). The thickness of shear bands in granular materials. Geotechnique, 37 (3), 271-283.

Ness, C. and Sun , J., (2015) Flow regime transitions in dense non-Brownian suspensions: Rheology, microstructural characterization, and constitutive modeling, Physical Review E 91, 012201

Oda, M., J. Konishi, S. Nemat-Nasser, (1982) Experimental micromechanical evaluation of strength of granular materials: Effects of particle rolling, Mechanics of Materials 1 (4) 269-283.

Ostojic, S., Somfai, E., & Nienhuis, B. (2006). Scale invariance and universality of force networks in static granular matter. Nature, 439(7078), 828-830.

Owens, EI. and Daniels, KE, (2013), The effect of force chains on granular acoustics, Soft Matter, 2013, 9, 1214.

Radjai, F., Jean, M., Moreau, J. J., & Roux, S. (1996). Force distributions in dense two-dimensional granular systems. Physical review letters, 77(2), 274. doi:10.1103/PhysRevLett.77.274

Radjai, F., Roux, S., & Moreau, J. J. (1999). Contact forces in a granular packing. Chaos: An Interdisciplinary Journal of Nonlinear Science, 9(3), 544-550.

Radjai, F., Wolf, D. E., Jean, M., & Moreau, J. J. (1998). Bimodal character of stress transmission in granular packings. Physical Review Letters, 80(1), 61, doi:10.1103/PhysRevLett.80.61

Roscoe, K. H. (1970), The influence of strains in soil mechanics. Geotechnique, 20 (2), 129-170.

Taboada, A., Chang,Kj., Malavieille J., (2005), Observations and simulation of force transmission in deformed conglomerates (Jiu-Jiu Fon, Taiwan) in Powders and Grains: 5th International Conference on Micromechanics of Granular Media, Stuttgart, vol. 1, edited by R. Garcıa-Rojo, H. J. Herrmann, and S. McNamara, pp. 73–75, A. A. Balkema, Brookfield, Vermont.

Vinutha, HA and S. Sastry, (2019), Force networks and jamming in shear-deformed sphere packings, Phys. rev. E, 99, 012123

# Figure captions

*[Figure 1. DEM model]*
3D numerical model of granular shear using discrete element method (DEM). Unbonded particles that make up the granular 'gouge' (shaded light grey) and the upper and lower boundary particles (shaded dark grey) are shown. Constant normal stress is applied to upper and lower boundaries in the z-direction (vertical) and shear is applied in the x-direction with sense of shear indicated by arrows. Repeating boundaries are used right and left, and frictionless walls front and back.

*[Figure 2. Contact forces]*
Snapshot of contact forces developed in a typical granular shearing simulation after engineering shear strain = 1 (i.e. shear strain 100%) plotted for a x-z plane of a 3D simulation (modified after Mair and Hazzard, 2007). Shearing direction is indicated by arrows. Contact forces between neighbouring particles are represented as cylinders. Their width, length and orientation represent the force magnitude (in Newtons) and the orientation of total contact force acting between adjacent particles. Larger forces are plotted as wider, lighter coloured cylinders. There is a preferred orientation of larger forces into two main 'chains' or clusters oriented obliquely to the shearing direction that carry enhanced force across the granular layer from upper to lower boundary of the model. Orientations of contact forces are presented in Figure 5.

*[Figure 3. Percolation]*
This figure shows the population of strong contact forces represented as cylinders for the initial stages of a simulation after normal stress has been applied (vertically) but before any shearing has taken place. A force cluster that percolates the system from upper to lower boundaries (red) and non-percolating contact force network (white) is highlighted. If the force F between two particles exceeds (or equals) a threshold value $F_t$, it is included in the network. The resulting network is defined as percolating if it connects the upper and lower boundaries of the model. $F_c$, the percolation threshold, is the maximum value of $F_t$ where a network first percolates.

*[Figure 4. Macroscopic friction]*
Macroscopic friction (shear stress/ normal stress) measured at the upper and lower boundaries of the model is plotted versus shear strain. The model (om015) presented has gaussian particle size distribution (psd) and constant applied normal stress of 15 MPa. Similar data for other simulations is summarised in Table 1. The red box indicates the period of the data to be presented in more detail in Figures 5 and 6.

*[Figure 5. Contact force orientations]*
Orientations of the strong contact forces i.e. all forces with $F/F_{mean} > 1$ are now presented for the simulation shown in Figure 4. Contact force orientations, weighted by force magnitude, are plotted as polar histograms. Data are projected onto (a) x-z plane exposing shear direction (top to left, see black arrows) and (b) the perpendicular x-y plane respectively. The data presented are for 50 increments of increasing shear strain from shear strains of 0.66 to 0.8 as indicated by the greyscale colourbar (from dark to light). This is the period indicated by the red box in Figure 4. The red and blue arrows highlight the start and end of this period respectively. This specific period is further analysed in Figure 6.

*[Figure 6a. Friction and percolating clusters]*
In Figure 6a we plot simple structural measures from the percolating cluster alongside macroscopic friction versus shear strain for period from 0.66 to 0.8 shear strain (indicated in box, Figure 4) covering a fluctuation in friction. The number of particles increases dramatically at a drop in friction indicating that dominant force network becomes temporarily more diffuse, before returning to a focussed and directed network indicated by the small number of particles in the chain.

*[Figure 6b. Percolating threshold and clusters]*
In Figure 6b we show the relationship between $F_c$, the percolating threshold force, and the structure of the percolating network quantified as number of particles involved in the percolating cluster for the same period as Figure 6a. $F_c$ is relative measurement (quoted as $F/F_{max}$) collected for each snapshot. The data show an inverse relationship, indicating that magnitude of contact forces in the percolating chain decrease as it becomes more diffuse at a drop in friction (shown in Figure 6a). Similar Percolating threshold data for other simulations is presented in Table 2.

*[Figure 7. Topology of percolating clusters - narrow psd]*
The 3D structure of the percolating clusters i.e. strong contact forces that make up the important (connected) system spanning force networks, are plotted here for a granular shear simulation having a narrow (gaussian) particle size distribution. Data are plotted in side view (z-x plane) in the left column (a, c, e, g, i) and viewed from above (y-x plane) in the right column (b, d, f, h, j), with each row representing equivalent data but just viewed from a different orientation. Shearing direction in all images is top to the left as indicated by the arrows (a). Data are plotted for a snapshot at engineering shear strain = 1. Cylinders representing the force with their width, length and orientation representing the magnitude, distance between particle centres and direction respectively. Figures (a) & (b) highlight the contact force network that first spans from top to bottom boundaries of the simulation just at the Percolating threshold $F_c = F_t = 0.329$. Note that due to the repeating boundaries in the model (right and left), although the network appears in two pieces, it exits right and re-enters on the left so comprises a single connected structure. In the subsequent rows of this figure (Figure 7c-j), we present the main system spanning networks that appear just above the percolating threshold (i.e. at Forces $F_t$ lower than $F_c$). The distinct colours signify distinct clusters of comprised of connected elements but not connected to each other. At $F_t = 0.309$, the original Fc cluster expands (Figure 7c-d) and 3 new distinct force networks blue (Figure 7e-f), red (Figure 7g-h), gold (Figure 7i-j) are identified. (Data is also presented as Animation A1)

*[Figure 8. Topology of percolating clusters - wide psd]*
The 3D structure of the percolating clusters i.e. strong contact forces that make up the important (connected) system spanning force networks, are plotted here for a granular shear simulation having a wide (power law) particle size distribution. Data are plotted in side view (z-x plane) in the left column (a, c, e) and viewed from above (y-x plane) in the right column (b, d, f), with each row representing equivalent data but just viewed from a different orientation. Shearing direction in all images is top to the left as indicated by the arrows (a). Data are plotted for a snapshot at engineering shear strain =1. Cylinders representing the force with their width, length

and orientation representing the magnitude, distance between particle centres and direction respectively. Figures (a) & (b) highlight the contact force network that first spans from top to bottom boundaries of the simulation just at the Percolating threshold $F_c = F_t = 0.216$. In the subsequent rows of this figure (Figure 8c-f), we present the main system spanning networks that appear just above the percolating threshold (i.e. at Forces $F_t$ slightly lower than $F_c$). The colour signifies connected elements, hence at $F_t = 0.196$ and $F_t = 0.176$, the original $F_c$ cluster systematically expands (Figure 7c-d, and e-f respectively) but no discrete new networks are formed. (This data is also presented as Animation A2)

# Tables

*[Table 1. Simulations and conditions]*

| simulation | psd | diameter | sigma n (MPa) | shear rate (micron/s) | friction (mean) | friction (stdev) |
|---|---|---|---|---|---|---|
| om014 | gaussian | 254 (22) | 5 | 0.0005 | 0.3768 | 0.139 |
| om013 | gaussian | 254 (22) | 15 | 0.0005 | 0.3605 | 0.0151 |
| om014_30 | gaussian | 254 (22) | 30 | 0.0005 | 0.3646 | 0.0164 |
| om016L | gaussian | 500 (44) | 5 | 0.0005 | 0.3927 | 0.0283 |
| om015 | gaussian | 500 (44) | 15 | 0.0005 | 0.3579 | 0.0246 |
| om017 | gaussian | 500 (44) | 30 | 0.0005 | 0.3605 | 0.0245 |
| om013v_0.00005 | gaussian | 254 (22) | 15 | 0.00005 | 0.2676 | 0.0160 |
| om015v_0.00005 | gaussian | 500 (44) | 15 | 0.00005 | 0.2864 | 0.0248 |
| om017v_0.05 | gaussian | 500 (44) | 30 | 0.05 | 0.6763 | 0.1101 |
| om017v_0.005 | gaussian | 500 (44) | 30 | 0.005 | 0.3858 | 0.0292 |
| om017 | gaussian | 500 (44) | 30 | 0.0005 | 0.3605 | 0.0245 |
| om017v_0.00005 | gaussian | 500 (44) | 30 | 0.00005 | 0.2939 | 0.0240 |
| tn032f | powerlaw | D = 2.6 | 5 | 0.0005 | 0.3473 | 0.0102 |
| tn014f | powerlaw | D = 2.6 | 5 | 0.0005 | 0.3489 | 0.0090 |

Simulations have the micro-properties: interparticle friction 0.5; poisson's ratio 0.25; shear modulus 22 GPa; initial porosity = ca 0.4. Particle diameter is quoted as mean diameter (and in brackets standard deviation) in microns. Shearing velocity is v = 0.0005 (except where specified ); Steady state friction is determined after 50000 timesteps. Total number of timesteps = 0.5M, 2M.

*[Table 2. Percolation measures]*

| | | Contact forces | | Percolation threshold | | | | Connectivity | |
|---|---|---|---|---|---|---|---|---|---|
| **simulation** | **snaps/ t_inc** | **F mean** | **F max** | **Fc (abs) mean** | **Fc (abs) stdev** | **Fc (rel) mean** | **Fc (rel) stdev** | **K+1 mean** | **K+1 stdev** |
| om014 | 10 / 50K | 0.00028 | 0.00826 | 0.00087 | 0.00006 | 0.10547 | 0.00761 | 1259 | 276 |
| om013 | 10 / 50K | 0.00067 | 0.00908 | 0.00261 | 0.00022 | 0.28281 | 0.03881 | 233 | 208 |
| om014_30 | 10 / 50K | 0.00133 | 0.02172 | 0.00465 | 0.00032 | 0.28301 | 0.05606 | 131 | 123 |
| om016L | 40 / 50K | 0.00187 | 0.03337 | 0.00447 | 0.00103 | 0.13408 | 0.03111 | 271 | 80 |
| om015 | 10 / 50K | 0.00379 | 0.03312 | 0.01144 | 0.00151 | 0.33174 | 0.03963 | 62 | 68 |
| om015L | 13 / 100K | 0.00369 | 0.03726 | 0.01119 | 0.00143 | 0.32474 | 0.05440 | 111 | 81 |
| om017 | 10 / 50K | 0.00636 | 0.06279 | 0.02052 | 0.00308 | 0.39912 | 0.08879 | 36 | 32 |
| om017L | 40 / 50K | 0.00631 | 0.06638 | 0.02196 | 0.00335 | 0.40593 | 0.06855 | 25 | 19 |
| om016c* | 50 / 1K | 0.00192 | 0.03332 | 0.00408 | 0.00067 | 0.12173 | 0.01975 | 307 | 61 |
| om016Lc* | 50 / 1K | 0.00185 | 0.03349 | 0.00436 | 0.00054 | 0.12977 | 0.01599 | 256 | 72 |
| om013c* | 50 / 1K | 0.00066 | 0.01086 | 0.00253 | 0.00013 | 0.28824 | 0.02256 | 135 | 106 |
| om015c* | 50 / 1K | 0.00363 | 0.03297 | 0.01170 | 0.00156 | 0.35679 | 0.04691 | 53 | 68 |
| om017c* | 50 / 1K | 0.00634 | 0.05088 | 0.02233 | 0.00310 | 0.46140 | 0.05407 | 19 | 10 |
| om017c_0.00005* | 30 / 1K | 0.00563 | 0.04371 | 0.02048 | 0.00136 | 0.46960 | 0.03230 | 21 | 4 |
| om013v_0.00005 | 10 / 50K | 0.00063 | 0.00828 | 0.00268 | 0.00032 | 0.32178 | 0.03927 | 179 | 192 |
| om015v_0.00005 | 10 / 50K | 0.00337 | 0.03411 | 0.01257 | 0.00275 | 0.36523 | 0.07734 | 90 | 81 |
| om017v_0.05 | 10 / 50K | 0.00733 | 0.09665 | 0.02959 | 0.02260 | 0.32256 | 0.05642 | 25 | 11 |
| om017v_0.005 | 10 / 50K | 0.00636 | 0.05607 | 0.02365 | 0.02072 | 0.41719 | 0.09484 | 19 | 11 |
| om017 | 10 / 50K | 0.00636 | 0.06279 | 0.02052 | 0.00308 | 0.39912 | 0.08879 | 36 | 32 |
| om017v_0.00005 | 10 / 50K | 0.00585 | 0.05324 | 0.02360 | 0.01875 | 0.50781 | 0.04829 | 18 | 9 |
| tn032f | 1 | | | | | | | | |
| tn014f | 1 | | | | | | | | |

Contact force magnitudes (F) are extracted for a series of snapshots (snap) from each simulation. Fmean and Fmax are the mean and maximum contact forces for series of snapshots (snap) collected at time increments (t_inc) indicated. $F_c$ (abs) and $F_c$ (rel) are the absolute (in terms of F) and relative (quoted as $F/F_{max}$) percolation thresholds respectively. $F_c$ mean and stdev are calculated for the series of snapshots indicated. K+1 = number of particles in chain (where K = connectivity). Mean and stdev for the snapshots indicated is presented. Contact force data highlighted by [c*] is force data intensively dumped out over a short period (e.g. 50 snapshots, dumped out every 1000 (1K) timesteps as opposed to 10 snapshots, extracted every 50000 (50K) timesteps.

## Supplementary Material

*A1: Animation topology tn021g*
Animation highlighting the 3D structure of the data presented and described Figure 7i & j. Plotted are percolating force networks identified at engineering shear strain =1 for a gaussian size distribution simulation. Force threshold is $F_t = 0.309$ (in the vicinity of the percolation threshold $F_c = F_t = 0.329$). Colours signify connected elements so different colours indicate distinct system spanning clusters that are not connected.

*A2: Animation topology tn032f*
Animation highlighting the 3D structure of the data presented and described Figure 8e & f. Plotted are percolating force networks identified at engineering shear strain =1 for a power law size distribution simulation. Force threshold is $F_t = 0.176$ (in the vicinity of the percolation threshold $F_c = F_t = 0.216$). The single colour signifies that the system spanning network consists of a single cluster.

*Figure S1:* Number of particles in percolating chain as a function of normal stress for a series of simulations conducted at 5, 15 30 MPa and for grain sizes 254 and 500 microns. Data are summarised as mean and standard deviation of the individual measurements made in each snapshot considered (table 2).

*Figure S2:* The mean values of of $F_c$ i.e. the percolating threshold force obtained for the set of snapshots are plotted along with maximum and mean contact force magnitude as a function of normal stress (5, 15 and 30 MPa) for a series of simulations having mean grain size 254 microns (upper row), 500 (lower row) respectively. In general, for all datasets, maximum, mean and percolating Force magnitude increases with normal stress. Data are absolute values (quoted in terms of F) and are plucked from a series of (between 10-40) snapshots throughout the simulations. $F_{mean}$ and $F_{max}$ are the mean and maximum contact forces for series of snapshots (snap) collected at time increments (t_inc) indicated. Simulations having larger grain size, have systematically larger contact Forces. The percolating threshold force is notably smaller than maximum force but always appears larger than mean Force magnitude for a given simulation. The amount by which $F_c$ exceeds $F_{mean}$, increases systematically with applied normal stress.

Figure 1

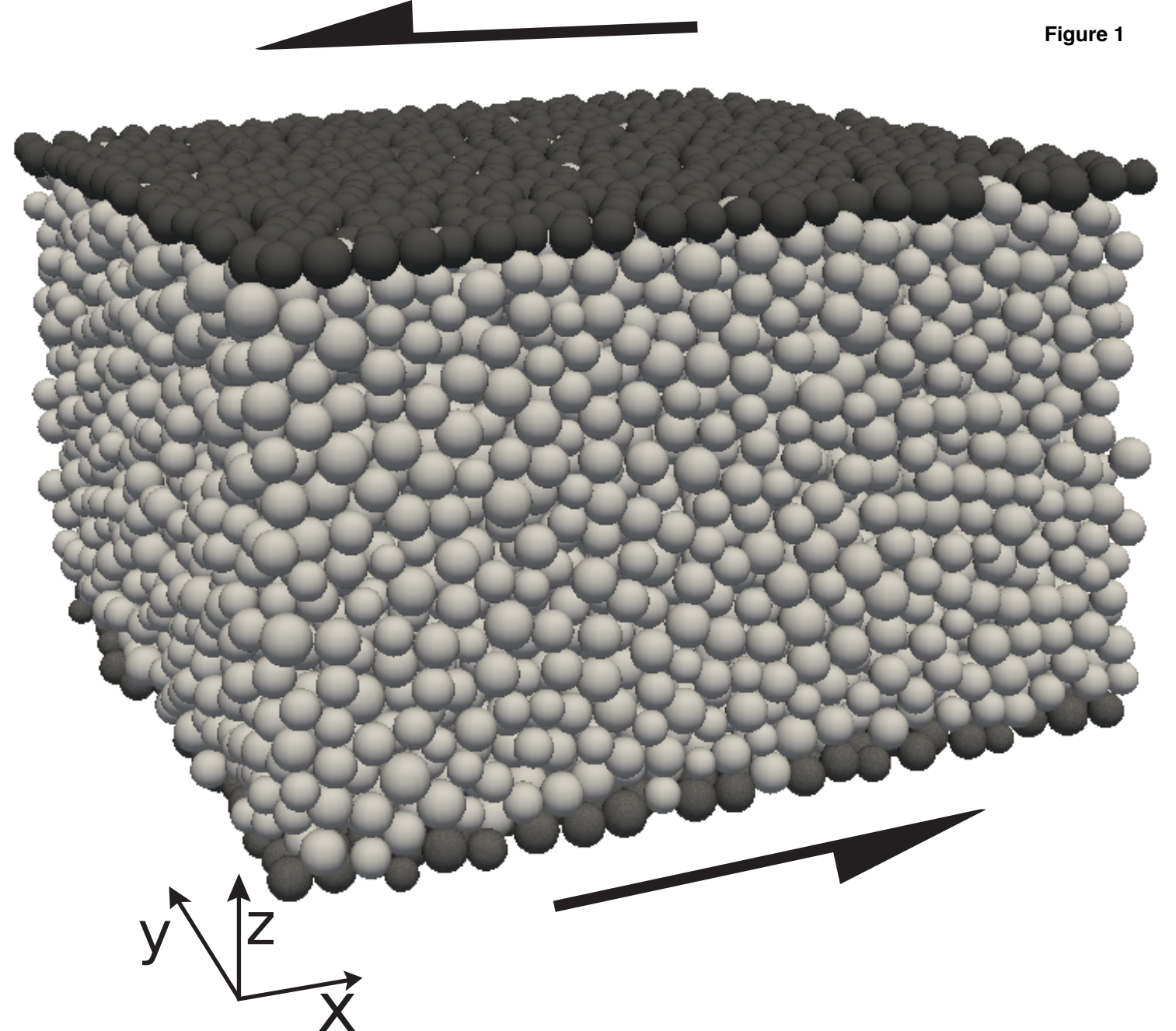

Figure 2

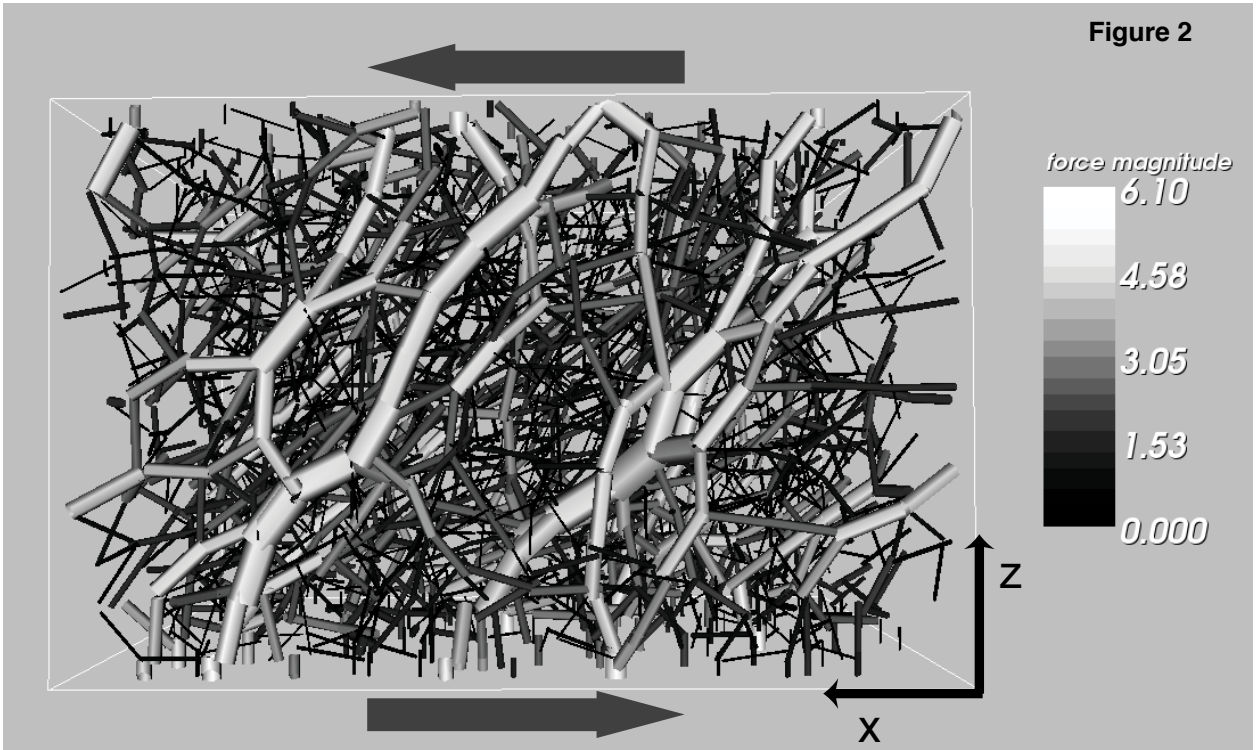

Figure 3

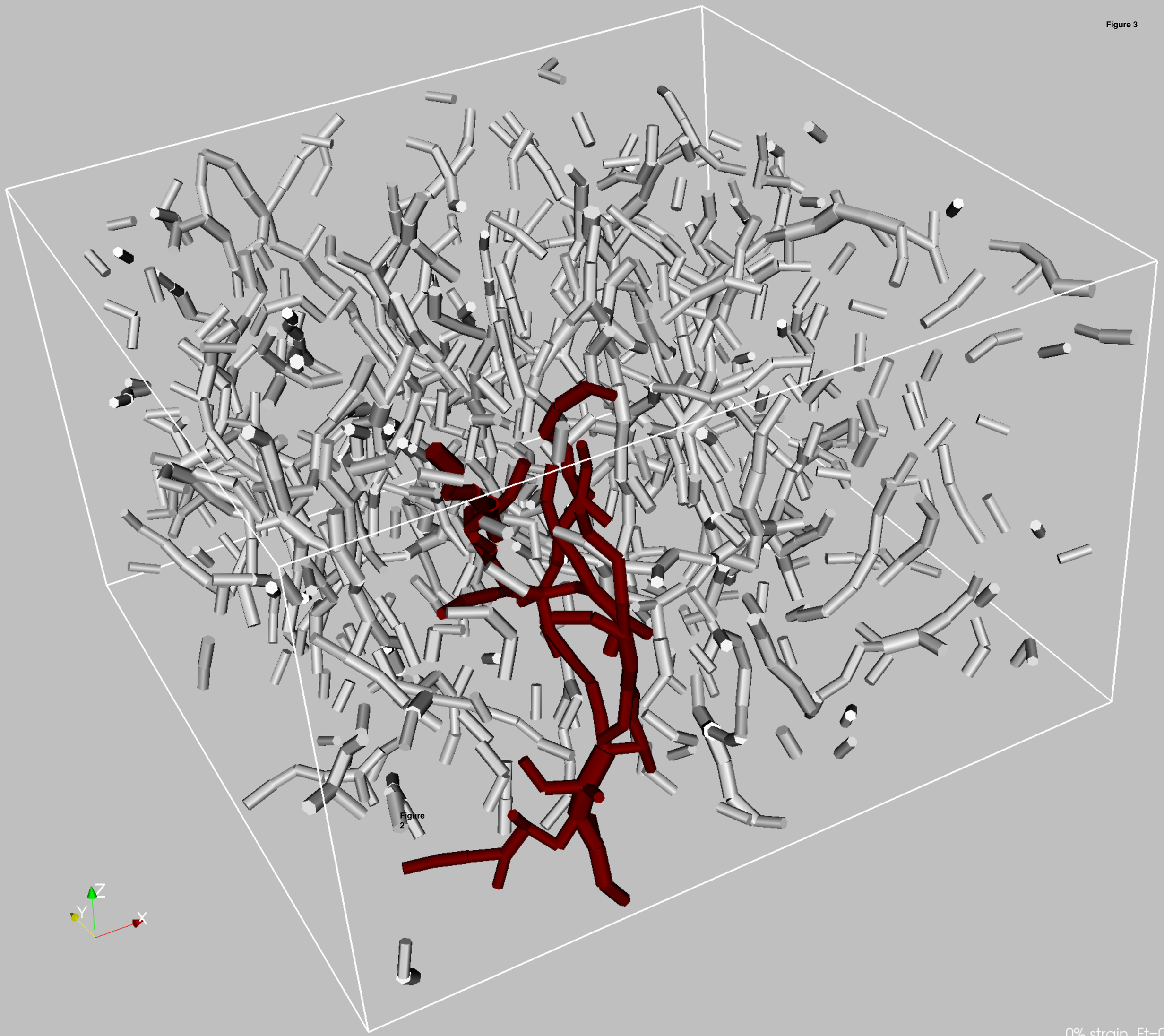

Figure 4

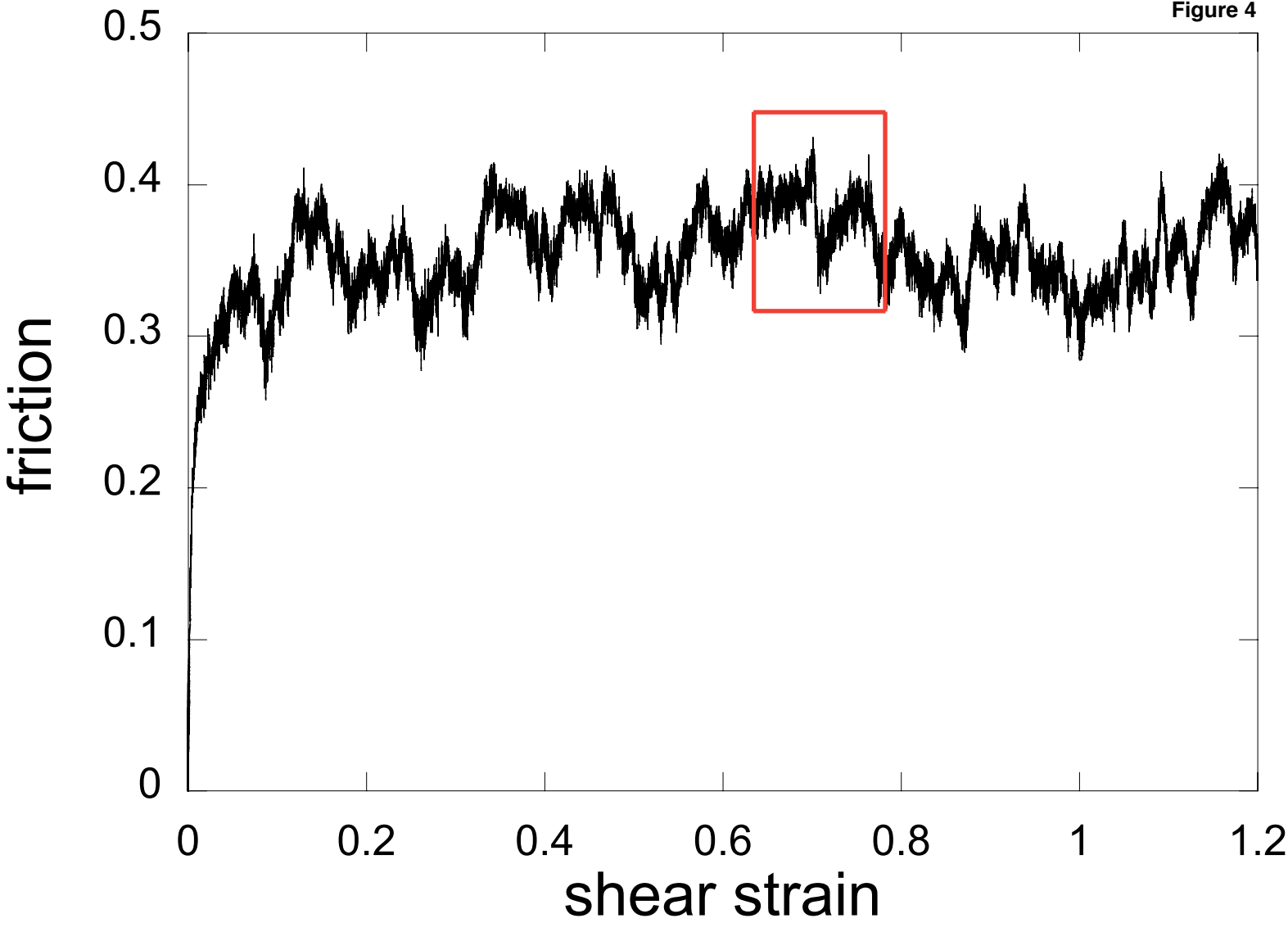

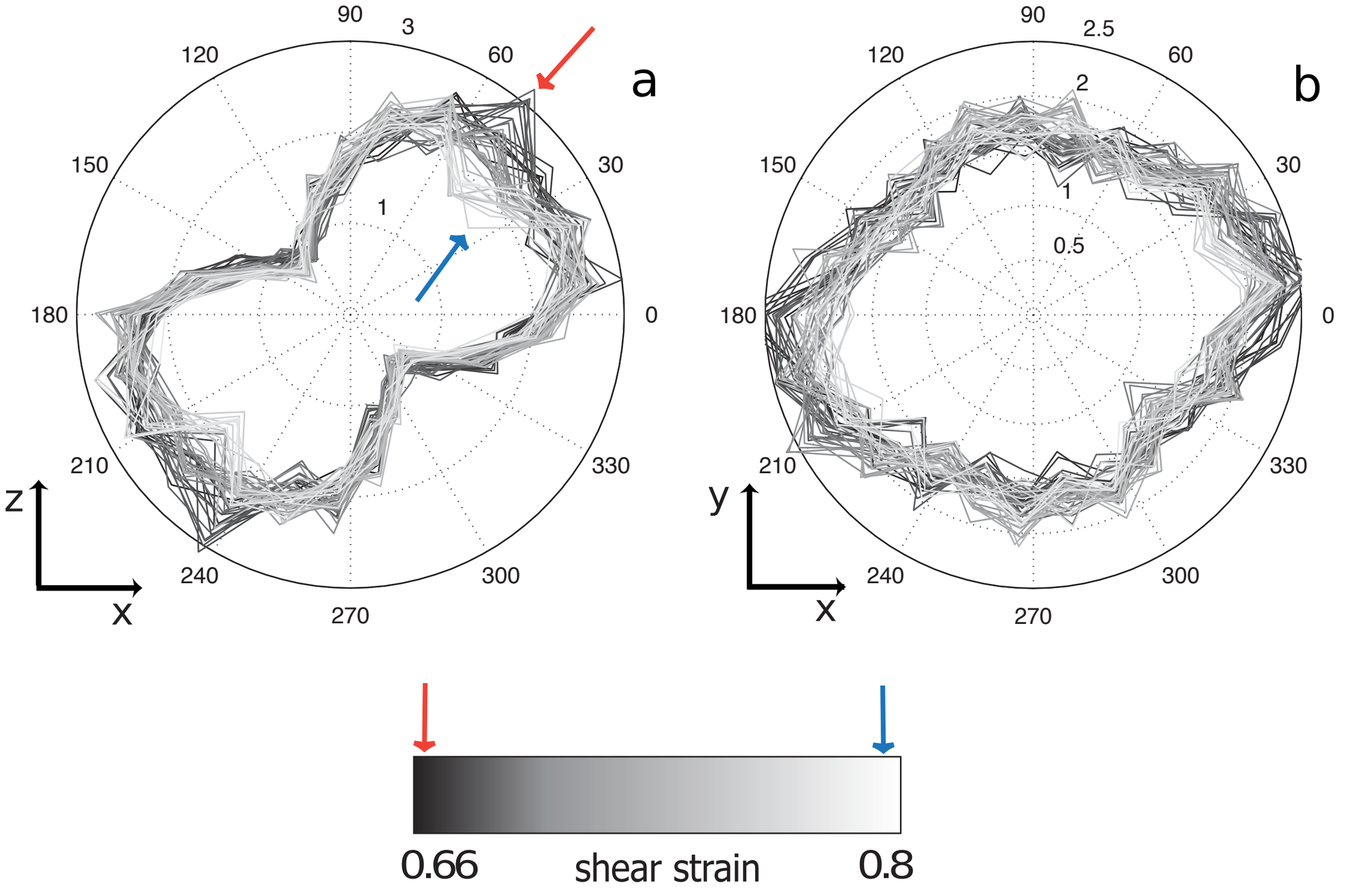
a
b
90
120
60
150
30
180
0
210
330
240
300
270
3
2.5
2
1
0.5
z
x
y
x
0.66
shear strain
0.8

**Figure 5**

Figure 6a

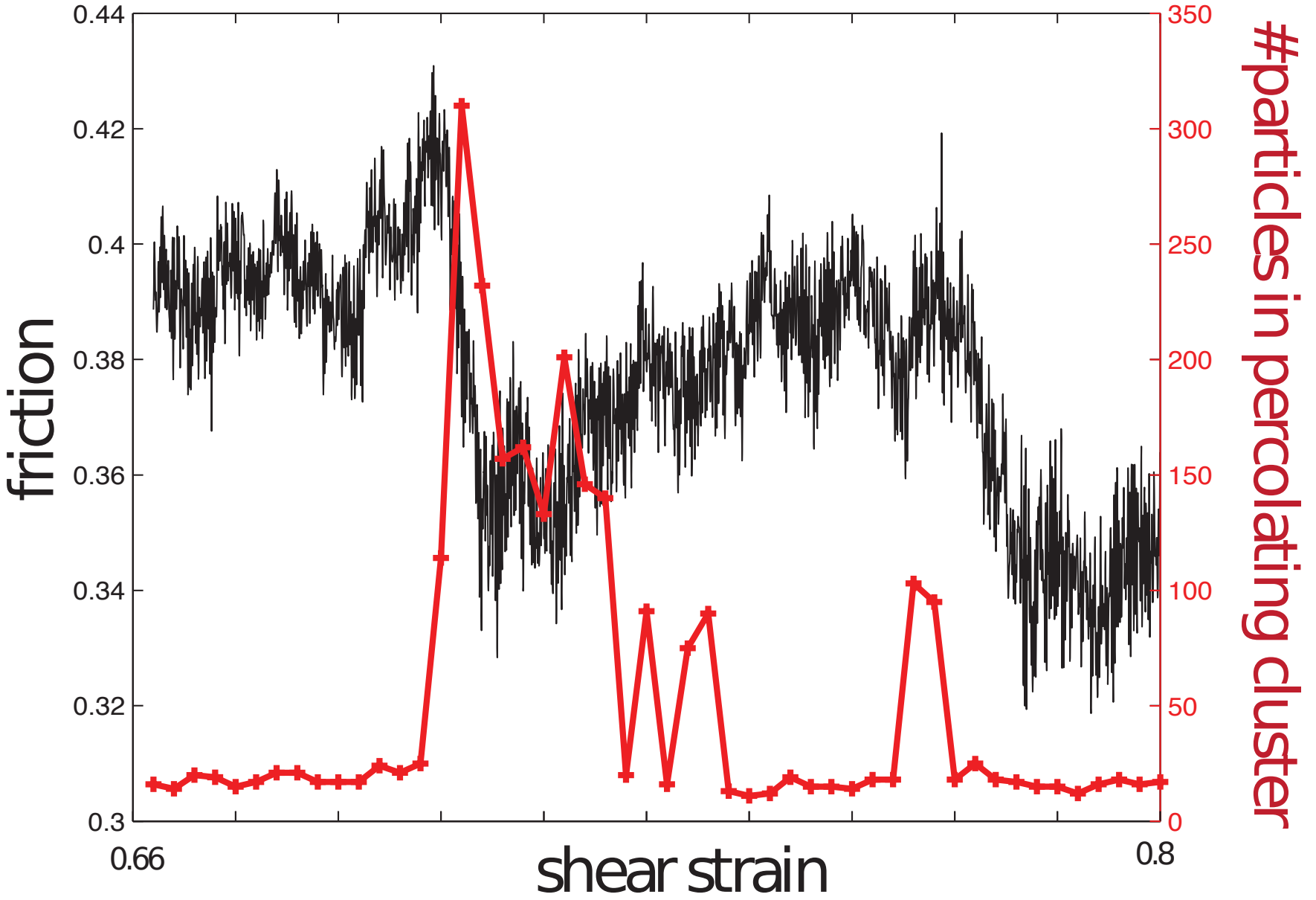
0.44
0.42
0.4
0.38
0.36
0.34
0.32
0.3
friction
0.66
0.8
shear strain
350
300
250
200
150
100
50
0
#particles in percolating cluster

Figure 6b

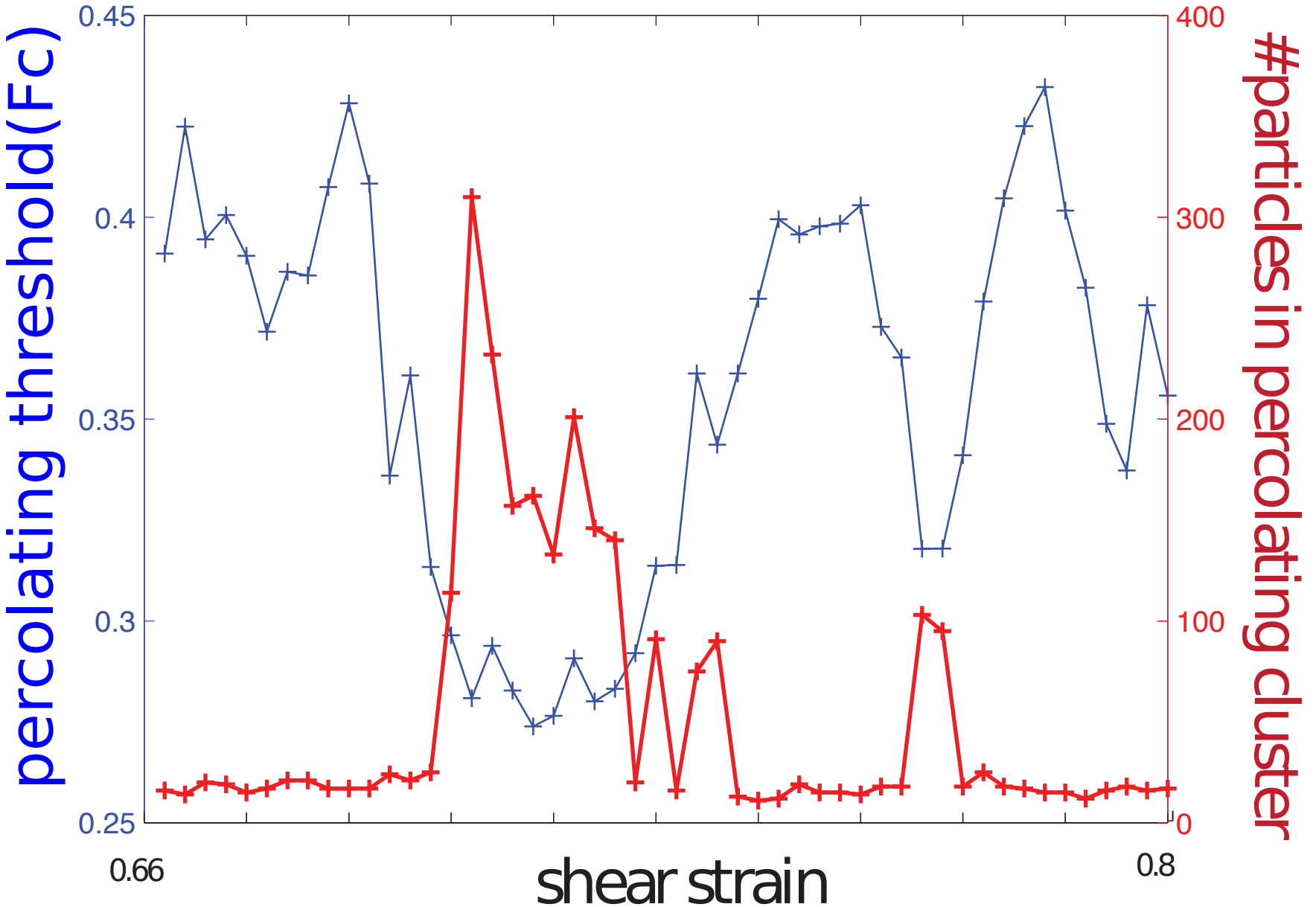
percolating threshold(Fc)
#particles in percolating cluster
shear strain
0.45
0.4
0.35
0.3
0.25
400
300
200
100
0
0.66
0.8

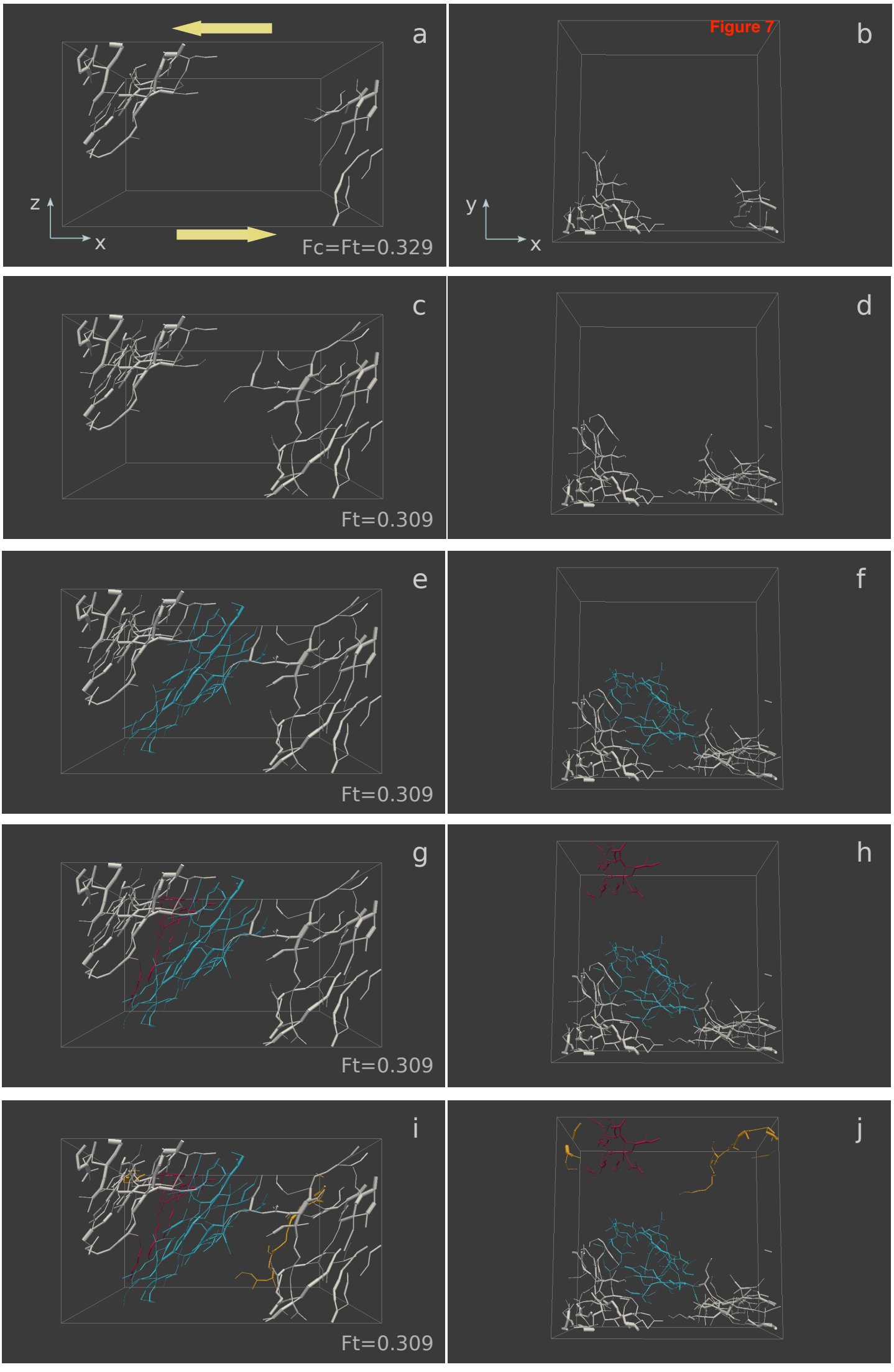
a
z
x
Fc=Ft=0.329
Figure 7
b
y
x
c
Ft=0.309
d
e
Ft=0.309
f
g
Ft=0.309
h
i
Ft=0.309
j

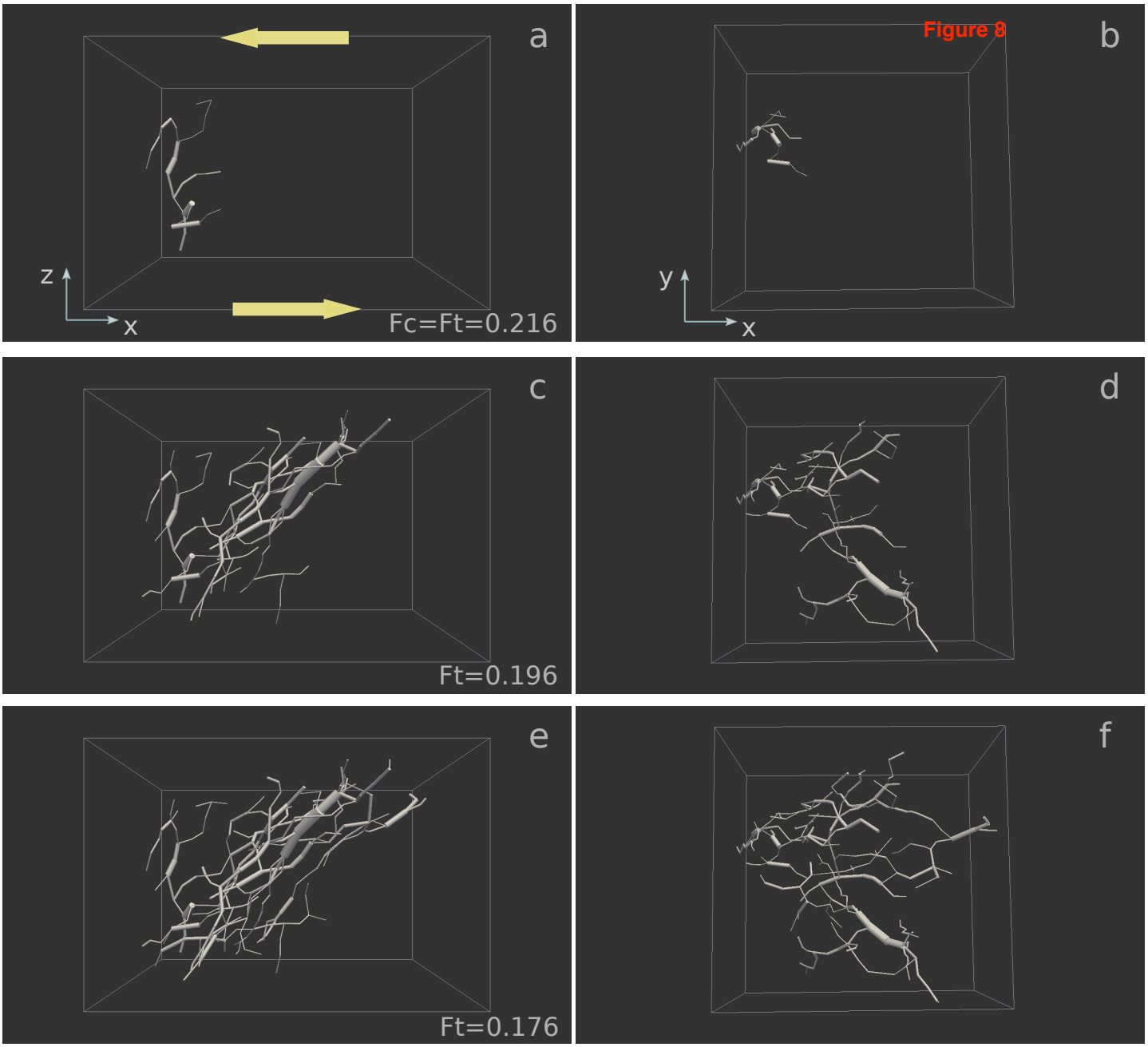
a
z
x
Fc=Ft=0.216
b
Figure 8
y
x
c
Ft=0.196
d
e
Ft=0.176
f

Figure S1


254 mean
254 stdev
500 mean
500 stdev
number of particles in percolating chain (K+1)
0
200
400
600
800
1000
1200
1400
normal stress MPa
0
5
10
15
20
25
30
35

Figure S2

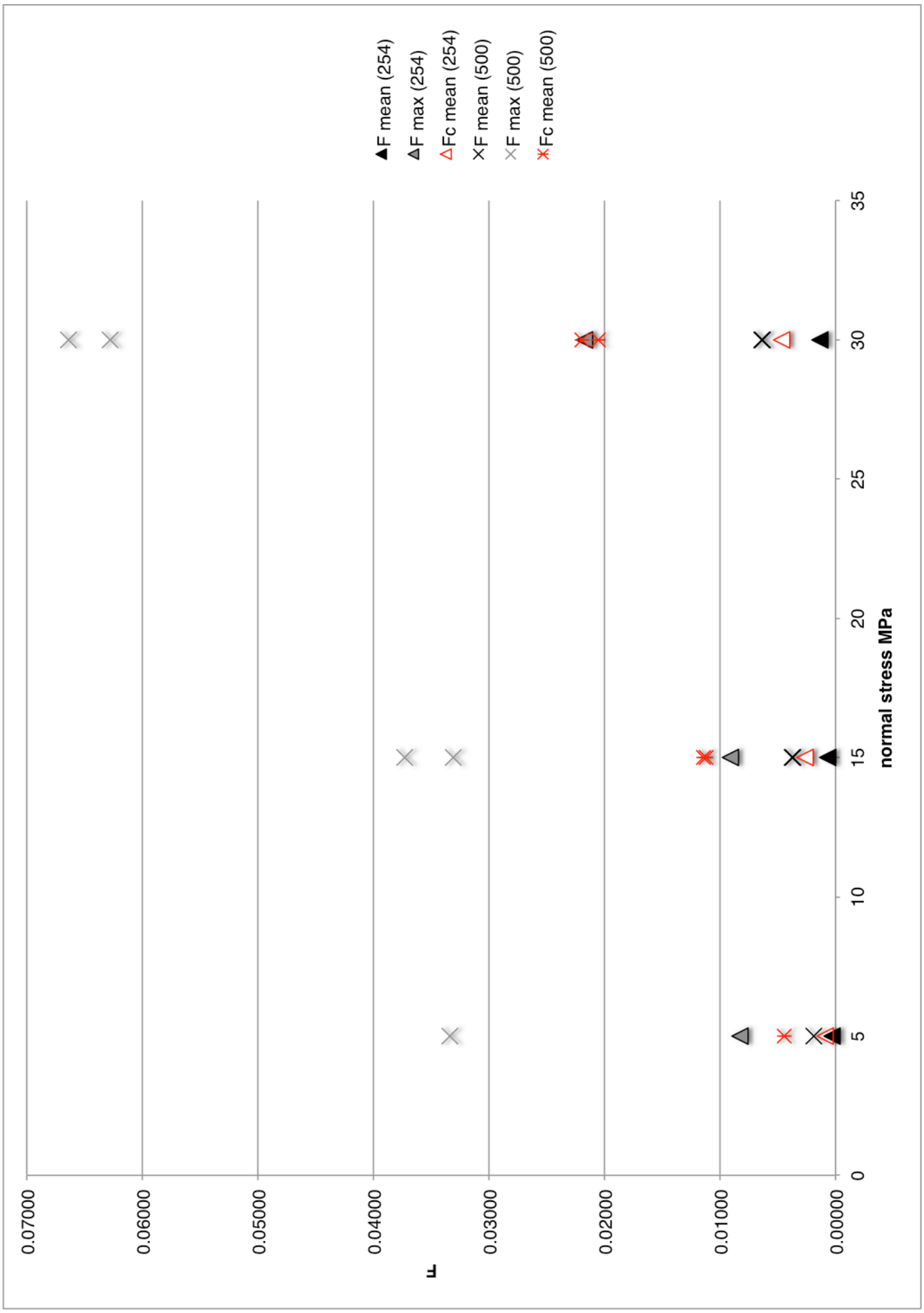
F mean (254)
F max (254)
Fc mean (254)
F mean (500)
F max (500)
Fc mean (500)
F
0.07000
0.06000
0.05000
0.04000
0.03000
0.02000
0.01000
0.00000
0
5
10
15
20
25
30
35
normal stress MPa